FEBS Letters 580 (2006) 3167–3172

para- and *ortho*-Pyridinium aldoximes in reaction with acetylthiocholine

Goran Šinko, Maja Čalić, Zrinka Kovarik*

Institute for Medical Research and Occupational Health, POB 291, HR-10 001 Zagreb, Croatia

Received 7 March 2006; revised 24 April 2006; accepted 25 April 2006

Available online 2 May 2006

Edited by Hans Eklund

Abstract In the oximolysis reaction *para*-aldoximes K027 and TMB-4 react faster with ATCh than *ortho*-aldoximes HI-6 and K033. The reaction rate constants at 25 °C were 22 M^{-1} min^{-1} for HI-6 and K033, 230 M^{-1} min^{-1} for TMB-4 and 306 M^{-1} min^{-1} for K027. Semi-empirical calculations showed that differences in rates do not origin from different electron density on the oxygen of the oxime group, but can be explained by the steric hindrance of the oxime group within the molecule. Thermodynamic parameters, $\Delta G^{\#}$, $\Delta H^{\#}$ and $\Delta S^{\#}$, were also determined for oximolysis reaction.

Keywords: Pyridinium aldoxime; Oximolysis; Spectrophotometry; Titration; Dissociation constants; Conformational analysis

1. Introduction

Pyridinium aldoximes are being tested as promising reactivators of phosphonylated acetylcholinesterase (AChE) (EC 3.1.1.7.) [1–3]. AChE has the key role in cholinergic neurotransmission and exposure to even small amounts of an organophosphorus (OP) compound (nerve warfare agents and some pesticides) can be fatal due to its inhibition by phosphylation. Only a few studies on the chemical and physical properties of aldoximes have been published by now [4–8] although a detailed understanding of the structural features of these compounds is an important step in the search for more effective antidotes.

We investigated structural features of two monopyridinium aldoximes, 1-(((4-carbamoylpyridinium-1-yl)methoxy)methyl)-2-((hydroxyimino)methyl)-pyridinium chloride (HI-6) and 4-carbamoyl-1-(3-(4-((hydroxyimino)methyl)pyridinium-1-yl)-propyl)pyridinium bromide (K027), and two bispyridinium aldoximes 1,1′-(propane-1,3-diyl)bis(4-((hydroxyimino)methyl)-pyridinium) bromide (TMB-4) and 1,1′-(butane-1,4-diyl)bis(2-((hydroxyimino)methyl)pyridinium) bromide (K033). HI-6 and TMB-4 are reactivators with well-known antidotal efficacy [1–3]. K027 and K033 are being evaluated as reactivators of phosphonylated AChE [9,10]. Conformational analysis was performed using molecular mechanics to determine the flexibility of the aldoxime molecules. The pH-dependant absorption spectra were determined for aldoximes and pK_a values were calculated. We evaluated the nucleophilic property of the oxime group of the aldoximes by studying their reaction with the AChE substrate acetylthiocholine iodide (ATCh) (oximolysis), because the mechanism of nucleophilic substitution by oxime is analogue to the aldoxime nucleophilic attack on both phosphylated AChE and ATCh [5]. Oximolysis was measured at different pH to confirm involvement of the oxime anion, oximate, in the nucleophilic attack. Thermodynamic parameters of oximolysis, $\Delta G^{\#}$, $\Delta H^{\#}$ and $\Delta S^{\#}$, were also evaluated because we found them useful for analyzing the structure–activity relationship for relative aldoxime reactivities.

2. Materials and methods

2.1. Chemicals and apparatus

Fig. 1 shows the structure of the studied aldoximes. K027 and K033 were supplied by Dr. Kamil Kuča (Department of Toxicology, Faculty of Military Health Sciences, Hradec Králové, Czech Republic). HI-6 was supplied by the Department for Organic Chemistry, Faculty of Science, University of Zagreb, Croatia. TMB-4 was synthesized in Bosnalijek, Bosnia and Hercegovina. ATCh was purchased from Fluka, Switzerland. Acetylcholine perchlorate (ACh) was purchased from BDH Chemicals, England. Experiments were done in 0.1 M sodium phosphate buffer ranging from pH 6 to 9.2. Solutions with pH above 9.2 were prepared with the addition of 0.2 M NaOH to 0.1 M Na_2HPO_4. Deionized water was used throughout. Aldoximes were dissolved in water, while ATCh and ACh in the buffer. Further dilutions were made in the buffer immediately before use. ATCh was 1, 2 and 5 mM, ACh was 20 mM and aldoximes were 0.1 mM in final concentration.

A SevenEasy pH-meter with an InLab® 413 electrode (both Mettler-Toledo GmbH, Switzerland) was used for pH measurements with the uncertainty of ±0.02 pH units. The pH-meter was calibrated at 25 °C using the two-point calibration method with commercially available Mettler–Toledo standard buffer solutions pH 7.00 and 9.21.

Aldoximes spectra were recorded at different pH on the Cary 300 spectrophotometer with temperature controller (Varian Inc., Australia) in 1 cm matched quartz cuvettes. Progress curves of oximolysis were measured with stopped-flow attachment SFA20-MX, equipped with a pneumatic drive (Hi-Tech Scientific, UK) on the Cary 300 spectrophotometer.

Conformational analysis was performed using molecular mechanics 2 (MM2) and semi-empirical calculations with MOPAC 2000 software (parameterized method 3 with conductor-like solvation model) created by J.J.P. Stewart (Fujitsu Ltd., Tokyo, Japan, 1999) according to published procedures [11,12].

*Corresponding author. Fax: +385 1 4673 303.
E-mail address: zkovarik@imi.hr (Z. Kovarik).

Abbreviations: AChE, acetylcholinesterase; ATCh, acetylthiocholine iodide; ACh, acetylcholine perchlorate; HI-6, 1-(((4-carbamoylpyridinium-1-yl)methoxy)methyl)-2-((hydroxyimino)methyl)pyridinium chloride; K033, 1,1′-(butane-1,4-diyl)bis(2-((hydroxyimino)methyl)-pyridinium) bromide; K027, 4-carbamoyl-1-(3-(4-((hydroxyimino)-methyl)pyridinium-1-yl)propyl)pyridinium bromide; TMB-4, 1,1′-(propane-1,3-diyl)bis(4-((hydroxyimino)methyl)pyridinium) bromide; OP, organophosphorus; MM2, molecular mechanics 2

0014-5793/$32.00
doi:10.1016/j.febslet.2006.04.070

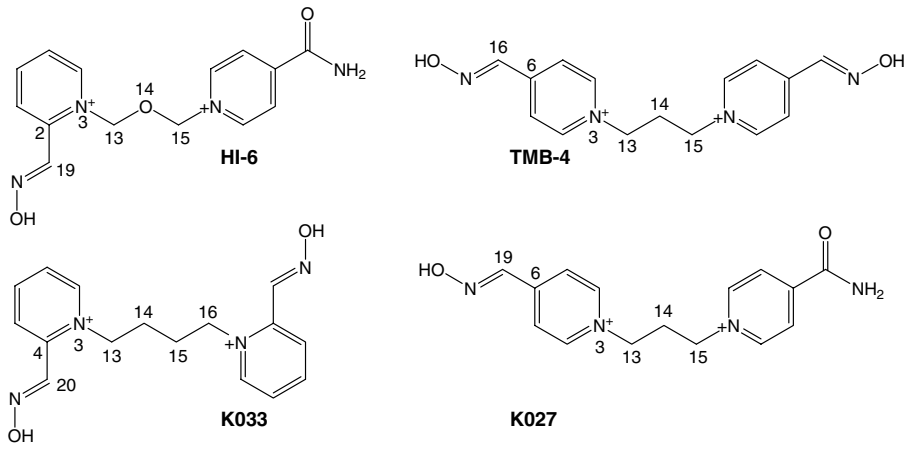

Fig. 1. Structural formulas of HI-6, K033, TMB-4 and K027.

$$H_2L^{2+} \overset{K_{a1}}{\rightleftharpoons} H + HL^{+} \overset{K_{a2}}{\rightleftharpoons} H + L$$

Fig. 2. Schematic representation of acid–base equilibriums in case of bisaldoximes.

2.2. Dissociation constants determination

Acid–base equilibrium (Fig. 2) is defined by the dissociation constant K_a. Bisaldoximes have two acid-base equilibriums, K_{a1} and K_{a2}. Constants were determined from pH-absorbance profiles at 25 °C using Eq. (1) for monoaldoximes and Eq. (2) for bisaldoximes as described earlier [13,14]

$$A_{tot} = \frac{A_2 \cdot [H^+] + A_3 \cdot K_{a1}}{[H^+] + K_{a1}} \quad (1)$$

$$A_{tot} = \frac{A_1 \cdot [H^+]^2 + A_2 \cdot [H^+] \cdot K_{a1} + A_3 \cdot K_{a1} \cdot K_{a2}}{[H^+]^2 + [H^+] \cdot K_{a1} + K_{a1} \cdot K_{a2}} \quad (2)$$

The observed absorbance at maximum absorption wavelength A_{tot} is the sum of the absorption fractions of all aldoxime ionization species present [13]. A_1, A_2 and A_3 are the absorbance of the pure diprotonated (H_2L^{2+}), monoprotonated (HL^+) and non-protonated (L) species, respectively. The concentration of hydrogen ions in medium is represented by $[H^+]$.

2.3. The oximolysis reaction constants

Fig. 3 shows the general scheme of reaction between the oximate and ATCh. At the wavelength of the maximum absorption of oximate, determined for each aldoxime, a decrease in oximate concentration was recorded, due to the reaction with ATCh (ACh). The oximolysis is defined by the equation:

$$v = \frac{dA_{tot}}{dt} = a \cdot (1 - e^{-k \cdot x \cdot b \cdot t}) \quad (3)$$

where the reaction rate (v) is absorbance changed per unit time and described by the second-order rate constant (k), ATCh (or ACh) concentration (b), and the oximate mole fraction (x) as the ratio of the concentration of the acetylated aldoxime (a) and the total concentration of aldoxime [15,16]. Oximolysis experiments were done at pH 7.4, 8.0, 8.5 and 9.2 using the stopped-flow method [17]. The progress curves of the oximolysis were transformed using the Lambert–Beer law from oximate absorbance into the concentration of formed acetylated aldoxime. The oximolysis was measured at three temperatures (12, 25 and 37 °C), and the energy of activation (E_a) was calculated from the corresponding second-order rate constants using non-linear regression by fitting the experimental data to the Arrhenius equation [17]. From

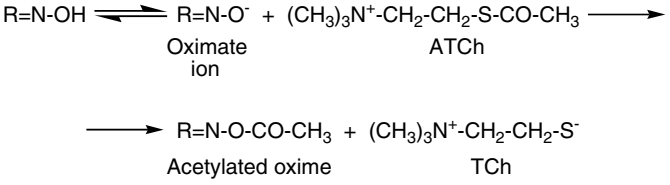

Fig. 3. Scheme of the oximolysis.

Table 1
Energy barriers (E) for rotation around single bonds in the aldoximes

Aldoxime	Pyridinium ring		Oxime group		Linker	
	Rotational bond	E (kcal/mol)	Rotational bond	E (kcal/mol)	Rotational bond	E (kcal/mol)
HI–6	N(3)–C(13)	15.0	C(2)–C(19)	6.0	C(13)–O(14);O(14)–C(15)	36.5;34.0
K033	N(3)–C(13)	7.1[a]	C(4)–C(20)	5.0[a]	C(13)–C(14);C(15)–C(16)	26.2[a]
K027	N(3)–C(13)	0.7	C(6)–C(19)	6.2	C(13)–C(14);C(14)–C(15)	27.6;27.3
TMB–4	N(3)–C(13)	0.7[a]	C(6)–C(16)	6.2[a]	C(13)–C(14);C(14)–C(15)	27.3[a]

[a]An average value due to the symmetry in the aldoxime molecule.

the obtained E_a and pre-exponential factor (A) we calculated the enthalpy ($\Delta H^{\#}$), entropy ($\Delta S^{\#}$) and Gibbs free energy ($\Delta G^{\#}$) of activation [17].

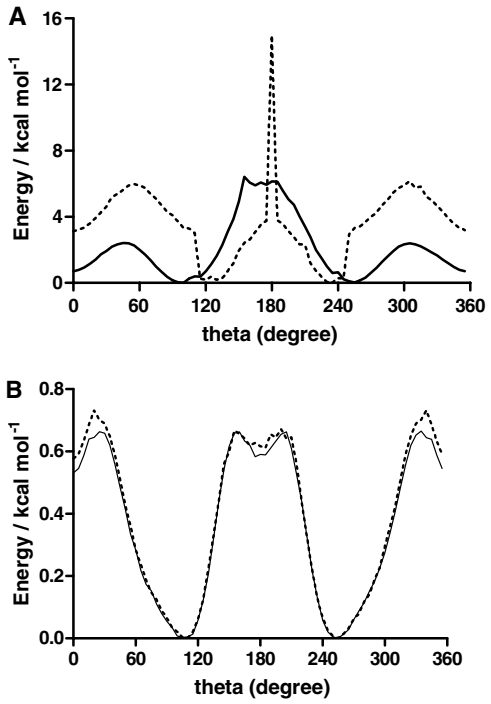

Fig. 4. Energy profile for rotation around N(3)–C(13) bond in the studied aldoximes. (A) Rotation for HI-6 (doted line) and K033 (solid line). (B) Rotation for K027 (doted line) and TMB-4 (solid line). Theta stands for dihedral angle in the aldoxime molecule and energies were calculated using the MM2 method.

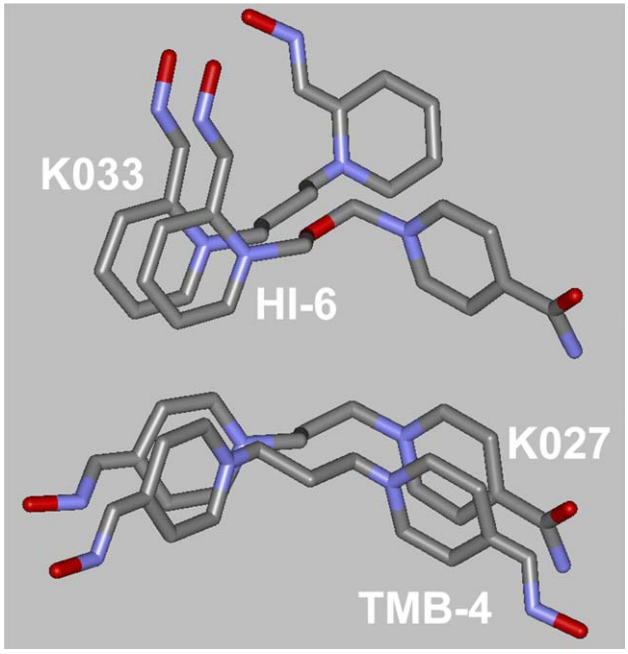

Fig. 5. Superposition of minimized structures of *ortho*- and *para*-aldoximes. Presented atoms are carbon (dark gray), nitrogen (blue), oxygen (red). Hydrogen atoms are not shown for better visibility.

3. Results and discussion

Since the flexibility of aldoxime molecule is important for binding to AChE, i.e. for its oxime group orientation towards phosphylated catalytic serine, we performed the conformational analysis of the aldoximes (Table 1). Pyridinium aldoximes with the oxime group in *para*-position, K027 and TMB-4, are more flexible than those with the oxime group in *ortho*-position, HI-6 and K033, due to the lower rotation barrier of the N(3)–C(13) bond (Fig. 4). A higher rotation barrier in *ortho*-pyridinium aldoximes is caused by the steric hindrance of the linker, which connects the two pyridinium rings. Moreover, bonds in the linker connecting atoms numbered 13 and 14, and atoms 14 and 15, determine the overall aldoxime rigidness resulted from the highest rotation energy barriers. Fig. 5 shows the superposition of the *ortho*- and *para*-aldoxime pairs and the spatial arrangement of the oxime groups bonded to the pyridinium rings. Semi-empirical calculations showed that the aldoximes had the similar electron density for protonated oxygen (−0.35) and for deprotonated oxygen (−0.89) in the oxime group.

The spectrophotometric measurements of the aldoximes spectra (200–500 nm, pH range between 6 and 10) showed two characteristic maximums in the UV region (Fig. 6). These maximums corresponded to the absorption of different aldoxime ionization forms as a result of $\pi \rightarrow \pi^*$ transitions within the pyridinium aldoxime aromatic system [18]. The maximum above 330 nm was a result of absorption of deprotonated pyridinium oxime group or groups, and were 344 nm for K027 and TMB-4, 337 nm for K033 and 354 nm for HI-6. The sharp isobestic point at 305 nm referred to the acid-base

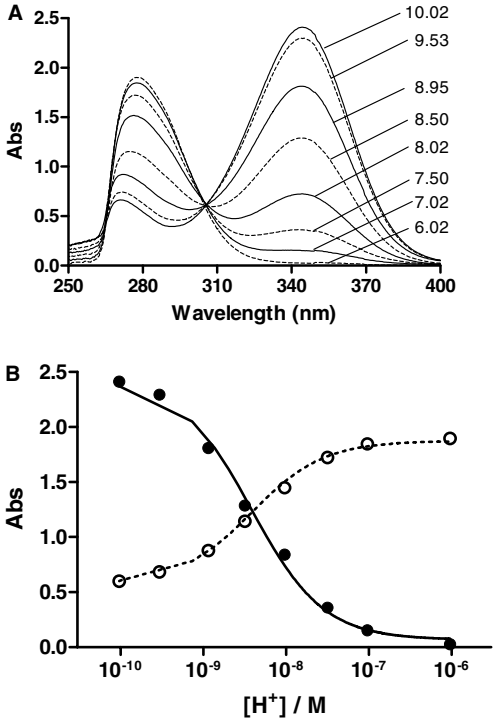

Fig. 6. Spectrophotometric determination of the aldoxime dissociation constant. (A) Absorption spectra of K027 (0.1 mM) at different pH (6.02-10.02). (B) Determination of K027 pK_a from the peak absorbance at various pH at 282 nm (○) and 344 nm (●). Solid and doted lines represent non-linear regression by Eq. (1).

equilibrium. Aldoxime dissociation constants were obtained from the absorbance maximums, for protonated and non-protonated ionic forms, by the non-linear fitting using Eq. (1) or (2) (Table 2), and pK_a values for HI-6 and TMB-4 were in good agreement with published values [1,4,13]. *ortho*-Pyridinium aldoximes HI-6 and K033 have a lower pK_a of the first equilibrium than *para*-pyridinium aldoximes K027 and TMB-4. Due to the lower pK_a, the simulation of the oximate pH-dependent concentration change showed higher oximate concentrations for HI-6 and K033 than for K027 and TMB-4 at physiological pH (Fig. 7).

In order to compare the nucleophilic potencies of the aldoximes, we measured the rates of reaction between aldoximes and thioester ATCh at different pH. Measurements performed at higher pH resulted in the increased observed rates of ATCh oximolysis. This effect was proportional to the increase in oximate concentration, thus confirming oximate involvement in the nucleophilic attack. This is in agreement with the pH-dependent HI-6 reactivation of phosphonylated AChE [19]. In the case of the oximolysis by bisaldoximes, we assumed that the two oxime groups were independent nucleophiles, which means that one mole of bisaldoximes can be treated as two moles of monoaldoximes. Since this was proved by our results (Fig. 8), the concentration of the formed acetylated aldoxime

Table 2
Dissociation constants (pK_a) for the aldoximes and the molar extinction coefficient (ε) of the diprotonated (H_2L^{2+}), monoprotonated (HL^+) and non-protonated (L) species of the oximes at 25 °C

Aldoxime	pK_{a1}	pK_{a2}	ε (M^{-1} cm^{-1})		
			H_2L^{2+}	HL^+	L
HI-6	7.47	–	–	389	15021
K033	7.48	8.46	375	15265	30901
K027	8.42	–	–	663	24302
TMB-4	8.39	9.51	0	26948	50088

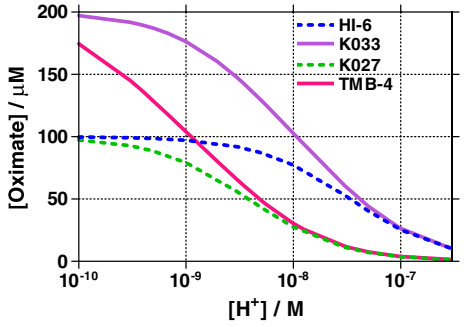

Fig. 7. The oximate concentration profile of the aldoximes at different acidities. Oximate concentrations for 0.1 mM aldoximes were calculated using Eqs. (1) and (2).

Table 3
Second-order rate constants (k) for ATCh oximolysis, expressed per oximate concentration, obtained by data analysis using the Eq. (3) for specified temperatures

Aldoxime	k (M^{-1} min^{-1})		
	12 °C	25 °C	37 °C
HI-6	8.11	22.1	47.0
K033	10.0	22.2	55.4
K027	135.0	305.6	756.6
TMB-4	95.6	231.4	595.9

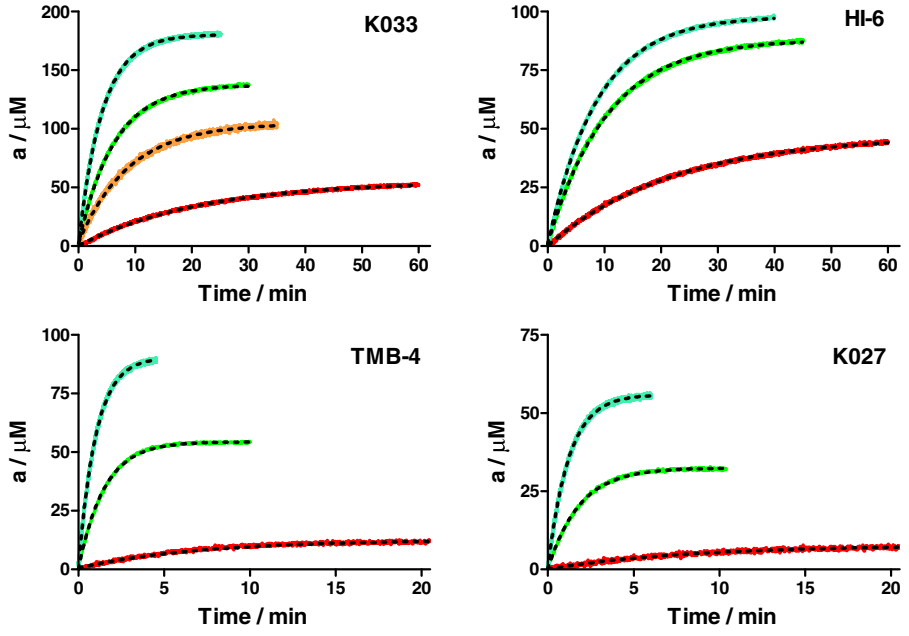

Fig. 8. Progress curves for ATCh oximolysis by aldoximes at 25 °C. Reactions were conducted at pH 7.4 (red), 8.0 (orange), 8.5 (green), and 9.2 (light blue). Black doted lines represent non-linear regression of simultaneous fit by Eq. (3). The initial concentration of the aldoximes was 100 μM, and of ATCh 5 mM. Reactions are followed up to the formation of about 90% of the acetylated aldoxime (a). Progress curve plateaus correspond to the concentration of oximate ions at cited pH. Oximolysis by K033 was also measured at pH 8 to test the independency of the oxime groups in reaction with ATCh. At this acidity, K033 should have a 100 μM oximate concentration (cf. Fig. 7), as it was confirmed with the orange progress curve plateau.

Table 4
Energy of activation (E_a) and pre-exponential factor (A) for ATCh oximolysis calculated from the Arrhenius equation for temperature range 12–37 °C

Oxime	E_a (kJ mol^{-1})	$A \times 10^8$ (M^{-1} s^{-1})	$\Delta G^{\#}$ (kJ mol^{-1})	$\Delta H^{\#}$ (kJ mol^{-1})	$\Delta S^{\#}$ (J K^{-1} mol^{-1})
HI-6	49.5	1.71	75.5	47.0	−95.6
K033	49.0	1.65	75.1	46.5	−95.9
K027	56.0	339	56.0	53.5	−51.6
TMB-4	64.0	1465	64.0	57.9	−39.5

Thermodynamic parameters for oximolysis at 25 °C, Gibbs free energy ($\Delta G^{\#}$), enthalpy ($\Delta H^{\#}$) and entropy ($\Delta S^{\#}$) of activation, were calculated using E_a and A [17].

was calculated according to the assumption. In order to calculate the second-order oximolysis rate constants (k) we used Eq. (3) for simultaneous fit of the progress curves obtained at different pH (Fig. 8, Table 3). The obtained constants, expressed per oximate concentration, showed that, at studied temperatures, aldoximes K027 and TMB-4 reacted at least 11 times faster with ATCh than HI-6 and K033. Semi-empirical calculations showed that the difference in rates did not origin from different electron density on the oxygen of the oxime group, but can be explained with the steric hindrance of the oxime group by the rest of the molecule. The oxime groups are more hindered in *ortho*- than in *para*-position, resulting in slower rates of ATCh oximolysis by HI-6 and K033.

From increase of oximolysis rate with increase of temperature, thermodynamic parameters were calculated using Arrhenius equation (Table 4) [17]. Free energy ($\Delta G^{\#}$) is an energy difference between the ground state and transition state, while both states depend on aldoxime structure. HI-6 and K033 had the highest free energy (75 kJ mol^{-1}) and K027 the lowest (56 kJ mol^{-1}). Probably due to steric constraints, the difference in the free energy between HI-6 and K027 of about 20 kJ mol^{-1} is the most significant, and therefore, the oximolysis rates for K027 were the highest. Thermodynamic parameters for HI-6 and K033 also indicated that these aldoximes reacted with ATCh in similar manner.

Since K027 has had the highest ATCh oximolysis rate, we tested its reaction with ACh, a physiological substrate of AChE, accumulated in OP poisoning due to the AChE inhibition. The experimental conditions (pH 9.2, 37 °C) were chosen to ensure a sufficient concentration of K027 oximate. The ACh oximolysis by K027 (k = 2 M^{-1} min^{-1}) was approximately 380 times lower than ATCh oximolysis. Therefore, the obtained rate is too slow and do not support the optional antidotal property of the aldoxime, confirming previously reported results [20,21]. The ACh oximolysis was not measured by other oximes, but based on ATCh results we assume that it would be even slower than 2 M^{-1} min^{-1} at pH 9.2, 37 °C. The oximolysis reaction is important especially during enzyme activity assay because it can interfere with enzyme ATCh hydrolysis.

Our study presented in this paper could help to analyze other aldoximes by their nucleophilicity and overall reactivity. However, one should keep in mind that the efficacy of aldoxime in AChE reactivation depends not only on its structure, but also on the structure of the OP inhibitor and the source of the enzyme [9,10,22,23].

Acknowledgements: We thank Dr. Kamil Kuča (Department of Toxicology, Faculty of Military Health Sciences, Hradec Králové, Czech Republic) for preparing and supplying the aldoximes K027 and K033. This work was supported by a NATO Reintegration Grant (EAP.RIG.981791) and by the Croatian Ministry of Science, Education and Sports.

References

[1] Gray, A.P. (1984) Design and structure–activity relationships of antidotes to organophosphorus anticholinesterase agents. Drug Metab. Rev. 15, 557–589.
[2] Dawson, R.M. (1994) Review of oximes available for treatment of nerve agent poisoning. J. Appl. Toxicol. 14, 317–331.
[3] Kassa, J. (2002) Review of oximes in the antidotal treatment of poisoning by organophosphorus nerve agents. J. Toxicol.- Clin. Toxic. 40, 803–816.
[4] Schoene, K. and Strake, E.-M. (1971) Reaktivierung von diäthylphosphoryl-acetylcholinestrase Affinität und reaktivität einiger pyridiniumoxime. Biochem. Pharmacol. 20, 1041–1051.
[5] Bunton, C.A., Gillitt, N.D. and Kumar, A. (1997) Solvent effects on reactions of hydroxide and oximate ions with phosphorus(V) esters. J. Phys. Org. Chem. 10, 221–228.
[6] Lovrić, J., Burger, N., Deljac, V. and Mihalić, Z. (1999) Spectrophotometric studies of some novel derivates of pyridinium chloride. Croat. Chem. Acta 72, 123–133.
[7] Castro, A.T. and Figueroa-Villar, J.D. (2002) Molecular structure, conformational analysis and charge distribution of pralidoxime: Ab initio and DFT studies. Int. J. Quantum Chem. 89, 135–146.
[8] Mager, P.P. and Weber, A. (2003) Structural bioinformatics and QSAR analysis applied to the acetylcholinesterase and bispyridinium aldoximes. Drug Des. Discov. 18, 127–150.
[9] Čalić, M., Lucić Vrdoljak, A., Radić, B., Jelić, D., Jun, D., Kuča, K. and Kovarik, Z. (2006) In vitro and in vivo evaluation of pyridinium oximes: mode of interaction with acetylcholinesterase, effect on tabun- and soman-poisoned mice and their cytotoxicity. Toxicology 219, 85–96.
[10] Petroianu, G.A., Arafat, K., Kuča, K. and Kassa, J. (2006) Five oximes (K-27, K-33, K-48, BI-6 and methoxime) in comparison with pralidoxime: in vitro reactivation of red blood cell acetylcholinesterase inhibited by paraoxon. J. Appl. Toxicol. 26, 64–71.
[11] Kovarik, Z., Bosak, A., Šinko, G. and Latas, T. (2003) Exploring active sites of cholinesterases by inhibition with bambuterol and haloxon. Croat. Chem. Acta 76, 63–67.
[12] Šinko, G., Bosak, A., Kovarik, Z. and Simeon-Rudolf, V. (2005) Structure–inhibition relationships in the interaction of butyrylcholinesterase with bambuterol, haloxon and their leaving groups. Chem.-Biol. Interact. 157–158, 421–423.
[13] Foretić, B. and Burger, N. (2004) The dissociation constants of 1,1′-bis(pyridinium-4-aldoxime)trimethylene dibromide. Monatsh. Chem. 135, 261–267.
[14] Čakar, M.M., Vasić, V.M., Petkovska, Lj.T., Stojić, D.Lj., Avramov-Ivić, M. and Milovanović, G.A. (1999) Spectrophotometric and electrochemical study of protolytic equilibria of some oximes-acetylcholinesterase reactivators. J. Pharm. Biomed. 20, 655–662.
[15] Stojan, J. and Pavlič, M.R. (1992) Velocity of Ellman's reaction and its implication for kinetic studies in the millisecond time range. Neurochem. Res. 17, 1207–1210.
[16] Goličnik, M., Šinko, G., Simeon-Rudolf, V., Grubič, Z. and Stojan, J. (2002) Kinetic model of ethopropazine interaction with horse serum butyrylcholinesterase and its docking into the active site. Arch. Biochem. Biophys. 398, 23–31.
[17] Fersht, A. (1998) Structure and Mechanism in Protein Science: A Guide to Enzyme Catalysis and Protein Folding, W.H. Freeman and Company, New York.
[18] Stern, E.S. and Timmons, C.J. (1970) Gillam and Stern's Introduction to Electronic Absorption Spectroscopy in Organic Chemistry, Edward Arnold Ltd., London, p. 149.

[19] Kovarik, Z., Radić, Z., Simeon-Rudolf, V., Reiner, E. and Taylor, P. (2005) Acetylcholinesterase mutants: oxime-assisted catalytic scavengers of organophosphonates. Chem.-Biol. Interact. 157-158, 388–390.
[20] Petroianu, G.A., Missler, A., Zuleger, K., Thyes, C., Ewald, V. and Maleck, W.H. (2004) Enzyme reactivator treatment in organophosphate exposure: clinical relevance of thiocholinesteratic activity of pralidoxime. J. Appl. Toxicol. 24, 429–435.
[21] Pannbacker, R.G. and Oehme, F.W. (2003) Pralidoxime hydrolysis of thiocholine esters. Vet. Human Toxicol. 45, 39–40.
[22] Worek, F., Thiermann, H., Szinicz, L. and Eyer, P. (2004) Kinetic analysis of interactions between human acetylcholinesterase, structurally different organophosphorus compounds and oximes. Biochem. Pharmacol. 68, 2237–2248.
[23] Kovarik, Z., Radić, Z., Berman, H.A., Simeon-Rudolf, V., Reiner, E. and Taylor, P. (2004) Mutant cholinesterases possessing enhanced capacity for reactivation of their phosphonylated conjugates. Biochemistry 43, 3222–3229.